Hindawi
Journal of Engineering
Volume 2019, Article ID 4292096, 11 pages
https://doi.org/10.1155/2019/4292096

Research Article

Using Bagasse and Aluminum Sulfate-Modified Bagasse as Adsorbents for Treatment of Industrial Cutting Fluid Wastewater in Laboratory and Pilot Scales

Natthaporn Pongtaveekan,[1] Piyapan Thammajaree,[1] Kowit Piyamongkala,[1] Nattaya Pongstabodee,[2] and Von Louie R. Manguiam[3]

[1]*Department of Industrial Chemistry, Faculty of Applied Science, King Mongkut's University of Technology North Bangkok, Bangkok, Thailand*
[2]*Department of Chemical Technology, Faculty of Science, Chulalongkorn University, Bangkok, Thailand*
[3]*School of Chemical, Biological, and Materials Engineering and Sciences, Mapúa University, Manila, Philippines*

Correspondence should be addressed to Kowit Piyamongkala; kowit.p@sci.kmutnb.ac.th

Received 23 May 2019; Revised 12 August 2019; Accepted 28 August 2019; Published 1 October 2019

Academic Editor: Dmitry Murzin

Industrial cutting fluid wastewater (CFW) is considered as hazardous substance due to its detrimental effects to the environment and workers welfare. Treatment of this type of wastewater was sometimes disregarded due to lack of knowledge and resources. However, adsorption, a straightforward approach, was used in this study to address this problem. The feasibility of the bagasse and modified bagasse in the adsorption of CFW was determined. Varying the adsorbent dosage resulted in an increase in the percent adsorption, whereas a decline for the adsorption capacity at equilibrium using a single-stage batch laboratory- and pilot-scale adsorption. The point of zero charge of the bagasse and the modified bagasse was measured to be at pH 5.5 and 2.4, respectively. The experiment also determined that, for a liter of CFW, 10.2 g and 59.2 g of the modified bagasse are required under laboratory- and pilot-scale systems, respectively. Isotherms of Langmuir, Freundlich, and Temkin were used in order to describe the adsorption process. It was determined that the surface heterogeneity and the pore size contributed to the adsorption of CFW; thus, Freundlich isotherm best fitted the data. Functional groups were verified using FTIR analysis and the heat of combustion, and their proximate analyses were determined. Based on the results under laboratory- and pilot-scale systems, modified bagasse is a viable material for the adsorption of CFW and solid fuel source.

1. Introduction

Cutting fluids, commonly known as metal working fluids, are used in several machining processes of turning, drilling, grinding, and milling to lubricate, dissipate heat, and flush fin chips [1]. These fluids also play a significant role in extending tool life and in increasing work quality outputs. In addition, these materials reduce wear and friction between assemblies. To start with, cutting fluids are divided into two types: oil- and water-based systems [2]. On the one hand, the oil-based materials or straight oil fluids are derived from animals, marine organisms, and vegetables. On the other hand, water-based oils can form an emulsion and are further divided into three classifications of synthetics, semi-synthetics, and soluble fluids. As per industrial preferences, water-based cutting fluids were mainly used for the following reasons: it can be used at high-speed cutting processes and high production at a relatively lower price. One of the main compositions of cutting fluids is mineral oils [3]. In addition, emulsifiers, surfactants, corrosion inhibitors, and biocides serve as additives to further enhance the properties of cutting fluids.

In the presence of thermal degradation, the applied cutting fluids lose their capability to lubricate. However, several factories are still using spent cutting fluids without considering the detrimental effects of these materials to tools

and for workers welfare. Spent cutting fluids are pungent gray-colored wastewater emulsion that can serve as a breeding ground for bacterial and fungal pathogens. When in contact, these pathogens will cause skin diseases such as skin rashes, dermatitis, and skin disorders and respiratory ailments, i.e., breathing problems, cough, chest tightness, asthma, and lung disease [4].

In order to address the problem of spent cutting fluids, various separation methods were devised which includes gravity settling, flotation, hydrothermal oxidation, membrane filtration, electroflotation, aerobic, anaerobic, and adsorption [5]. Among these methods, adsorption is one of the simplest yet unexplored knowledge on treating spent cutting fluids. Adsorption is a process that can operate at normal temperature and pressure. Additional of chemicals for deemulsion and adsorbent cleaning is not a requirement. According to several studies, cutting fluid, refinery effluent oil, crude, and mineral oil could be adsorbed by peat [6–8]. Solisio et al. used oxides of calcium and magnesium as adsorbents to treat exhaust oils [9]. Cambiella et al. used sawdust to address oil in water emulsion [10]. Piyamongkala et al. used modified chitosan to remove soluble cutting fluids [11]. Ibrahi et al. adsorbed mineral oil using modified barley straw [12]. Tembhurkar and Deshpande used lemon peels to treat cutting fluid [13].

In Thailand, sugar industry plays a significant role in agriculture. In the period of 2017-2018, about 134,930,000 tonnes of sugar were produced, generating a considerable amount of bagasse [14]. Bagasse is the by-product of sugar production from sugarcane. With these, bagasse becomes an ideal material in question for its application. Bagasse contains 46% cellulose, 24.5% hemicellulose, 19.9% lignin, 3.5% fat and waxes, 2.4% ash, 2% silica, and 1.7% other elements [15]. Consequently, it can be used as solid fuel for steam boilers. It was also found out that bagasse can be used as an adsorbent for the removal of dyes and heavy metals such as cadmium and zinc [16].

With the aforementioned capability of bagasse to adsorb certain materials, this paper intends to (i) study the feasibility of bagasse and modified bagasse to adsorb industrial cutting fluid wastewater using systems of laboratory and pilot scales, (ii) evaluate Langmuir, Freundlich, and Timken isotherms, (iii) predict the amount of adsorbent to volume of industrial cutting fluid wastewater ratio, and (iv) evaluate the capability of the spent adsorbent as solid fuel.

2. Materials and Methods

2.1. Adsorbate Collection. Industrial cutting fluid wastewater (CFW) collected was from an industry in Thailand which processed steel pipe, C-shaped, and plate machining works. Figure 1 shows the collected CFW. It has two layered solutions of lubricant oil (dark) and CFW (gray) emulsion. Several physical and chemical properties of CFW were determined such as temperature, 22°C; total suspended solid (TSS), 4,000 mg/L; pH level, 7.89; chemical oxygen demand (COD), 123,733.3 mg/L; and the oil and grease content of CFW, 535,033.3 mg/L.

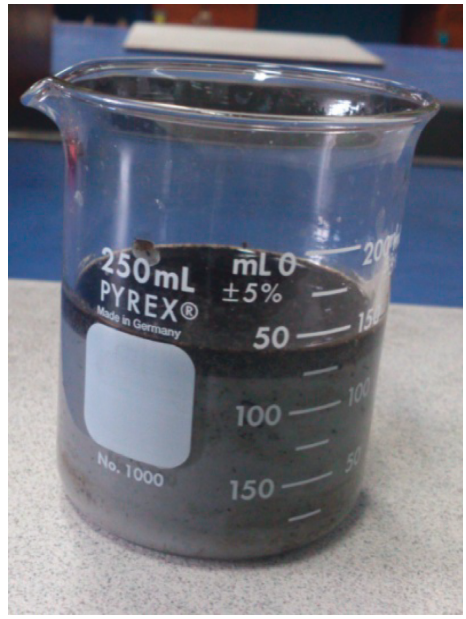

Figure 1: Industrial cutting fluid wastewater.

2.2. Adsorbent Preparation. The bagasse used in this study was obtained from a sugarcane refinery in Nakhon Sawan, Thailand. It was sun-dried for 48 hours followed by oven (Binder; Model FD 53) drying at 130°C for 3 hours. The dried bagasse underwent several measurements using the BET method (BEL JAPAN; Model Belsorp-mini) and found out to have a pore volume of 4.1×10^{-3} cm^3/g, a pore diameter of 38.2 nm, and a surface area of 4.1×10^{-1} m^2/g which was followed by modification. A 100 g of bagasse was reacted with a 1,000 cm^3 of 8% w/v commercial grade aluminum sulfate, stirred at 250 rpm for 4 hours. It was then screen filtered and oven-dried for 48 hours to obtain modified bagasse (MB) [17]. The pore volume, pore diameter, and surface area of the dried modified bagasse were also measured to be 9.2×10^{-3} cm^3/g, 69.4 nm, and 1.7×10^{-1} m^2/g, respectively. It was stored in an air-tight plastic container. Figure 2(a) shows the bagasse, and Figure 2(b) shows the modified bagasse.

2.3. Point of Zero Charge of the Adsorbent. The pH_{pzc} of bagasse and the modified bagasse was measured by preparing a solution of 0.10 M sodium chloride (BDH) with a pH value of between 1.0 and 11.0 using diluted hydrochloric acid (J. T. Baker) or sodium hydroxide (BDH) which followed the methods of Champreecha et al. [18]. A 0.1 g each of bagasse and modified bagasse was added in a separate 100 cm^3 salt solution, covered, and agitated by an orbital shaker (UMAC Scientific; Model UM-S60) at room temperature for 48 hours. The mixtures were then filtered through filter paper No. 1. The pH was measured and plotted against the initial pH. The pH that intersect the 45° line pH (initial) = pH (final) was taken as the point of zero charge of the adsorbents.

(a) (b)

Figure 2: Adsorbents: (a) bagasse and (b) modified bagasse.

2.4. Adsorption Experiment. Adsorption experiments were scaled to a laboratory and a pilot plant setup. All laboratory-scale batch adsorption experiments were carried out in a 250 cm^3 Erlenmeyer flasks. The adsorbent dosages (1.0–5.0 g) were added in a 100 cm^3 CFW. The emulsion was agitated at 120 rpm at room temperature. On the contrary, pilot-scale experiments were conducted in an 18 L of plastic tank containing CFW and the adsorbent (ranging from 200–1,000 g). The mixture was then over-head-stirred (IKA; Model RW 20 Digital) at room temperature set to 200 rpm. The residual concentration of the CFW was taken at equilibrium. The initial and residual concentrations of CFW were analyzed by a spectrophotometer (Thermo electron; Model Spectronic Genesys 20) at 395 nm [18]. The percent adsorption and adsorption capacity at equilibrium were calculated using equations (1) and (2), respectively. Figure 3 shows schematic diagram of the pilot-scale reactor.

$$\%\ \text{adsorption} = \left(\frac{C_0 - C_e}{C_0}\right) \times 100, \quad (1)$$

$$q_{e,\exp} = \left(\frac{(C_0 - C_e) \times V}{W}\right), \quad (2)$$

where C_0 is the initial concentration and C_e is the equilibrium concentration of the industrial cutting fluid wastewater (mg/L). $q_{e,\exp}$ is the experimental adsorption capacity at equilibrium (mg/g), V is the volume of the industrial cutting fluid wastewater (L),and W is the weight of the adsorbent (g).

2.5. SEM and Fourier-Transform Infrared Spectrometer. The surface morphology images of modified bagasse before and after adsorption of industrial cutting fluid were examined by scanning electron microscope (FEI, Model: Quanta 450) at 10 kV. The IR spectra of the CFW and modified bagasse before and after adsorption were analyzed by FTIR spectrometer (Perkin-Elmer; Model 2000) using a 4,000–400 cm^{-1} range. The samples were pulverized and mixed with potassium bromide (BDH) followed by pelletizing. The average of 10 scans was made having 4 cm^{-1} for its resolution.

2.6. Heat of Combustion and Proximate Analysis. The adsorbents (before and after adsorption) were used as solid fuel.

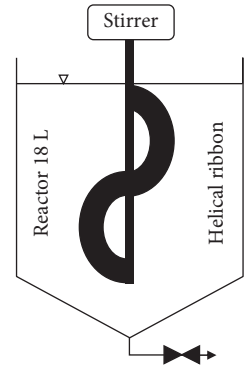

Figure 3: Schematic diagram of the pilot-scale reactor.

The heat gross calorific value and the proximate analysis of moisture, volatile, and ash were determined following ASTM D5865, E781, E872, and E1755, respectively. The fixed carbon content of the adsorbents was calculated after determining all the parameters using proximate analysis.

3. Results and Discussion

3.1. Point of Zero Charge. Bagasse is a biomass that contains complex organic components of proteins, lipids, and carbohydrates and from these, such pendant groups of hydroxyl and carboxylic can serve as possible sites for adsorption [19]. Equations (3) and (4) show the hypothetical adsorption reaction of the negatively charged CFW to a partial positively charged bagasse. The percent adsorption is a function of the adsorbent dosage which dictates the number of positive charge in an emulsion. In analogy, increasing the adsorbent dosage will result in an increase in positively charged molecules, thus increasing the percent adsorption:

$$(\text{bagasse} - \text{OH}) + \text{CFW}^- \rightleftharpoons \text{bagasse} - \text{O} - \text{CFW} + \text{H}^+ \quad (3)$$

$$(\text{bagasse} - \text{COOH}) + \text{CFW}^- \rightleftharpoons \text{bagasse} - \text{COO} - \text{CFW} + \text{H}^+ \quad (4)$$

One way to enhance the adsorptive properties of the adsorbent is by modification. In this study, the effect of introducing aluminum ions to the bagasse molecule was investigated. Equation (5) is the dissociation of aluminum

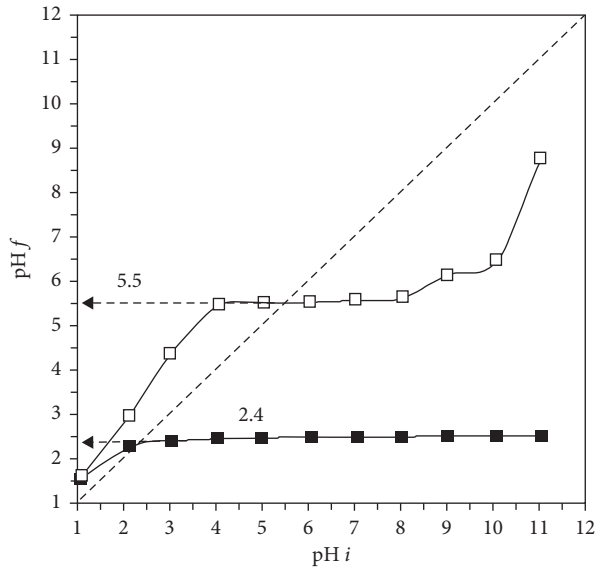

Figure 4: Point of zero charge of the adsorbents: bagasse (□) and modified bagasse (■).

sulfate to its ions. Equations (6) and (7) are the hypothetical modification reaction of bagasse with aluminum ion, and it was the basis for the determination of pH_{pzc} of the molecule. The additional positive charge from the aluminum ion can destabilize the negatively charged CFW by electrostatic attraction, chemical force, and adsorption [20]. On the contrary, equation (8) is the hypothetical adsorption of CFW to the modified bagasse molecule:

$$Al_2(SO_4)_3 \rightleftharpoons 2Al^{3+} + 3SO_4^{2-} \tag{5}$$

$$\begin{aligned}&(\text{bagasse} - \text{OH}) + Al^{3+} \rightleftharpoons (\text{bagasse} - \text{O} - Al^{n+})^{*} + H^{+}\\ &{}^{*}(\text{bagasse} - \text{O} - Al^{n+}) = \text{modified bagasse}\end{aligned} \tag{6}$$

$$\begin{aligned}&(\text{bagasse} - \text{COOH}) + Al^{3+} \rightleftharpoons (\text{bagasse} - \text{COO} - Al^{n+})^{**} + H^{+}\\ &{}^{**}(\text{bagasse} - \text{COO} - Al^{n+}) = \text{modified bagasse}\end{aligned} \tag{7}$$

$$(\text{modified bagasse}^{n+}) + n\text{CFW}^{-} \rightleftharpoons \text{modified bagasse} - (\text{CFW})_n \tag{8}$$

The functional groups present in the adsorbent significantly influence pH_{pzc} of the solution. Thus, depending on the pH of the solution, their surfaces might be positively charged, negatively charged, or electrically neutral when the solution pH is below, above, or equal to pH_{pzc}, respectively [21]. At $pH < pH_{pzc}$, the surface of the adsorbent has a net positive charge, whereas at $pH > pH_{pzc}$, the surface has a net negative charge. Figure 4 shows the pH drift test. The pH_{pzc} of the bagasse and the modified bagasse was determined to be at 5.5 and 2.4, respectively. Based from these values, modifying the bagasse surface will have a contributing factor on the adsorption of CFW.

Cutting fluids contain additives which are organic-based molecules that are ionic and nonionic moieties of amine, fatty acid, ester, sulfonates, soap, borate, and phosphate [22]. Based on the past research studies, pH_{pzc} of the cutting fluid was determined at pH 3.2 [11]. If the pH of the cutting fluid is above pH 3.2, the surface is negatively charged whereas positively charged if the pH is below the value of pH_{pzc}.

3.2. Effect of Adsorbent Dosage. Figures 5(a), 5(b), and 6 show the graphical relationship of percent adsorption, adsorbent dosage, and adsorption capacity at equilibrium using the systems of laboratory-scale bagasse and modified bagasse and pilot-scale modified bagasse, respectively.

As the adsorbent amount increases from 1.0 to 5.0 g (laboratory scale) and 200 to 1,000 g (pilot scale), the percent adsorption also increases (1.5–2.4% for bagasse under laboratory scale; 86.9–97% for modified bagasse under laboratory scale; and 100% for modified bagasse under pilot scale). Increasing the amount of adsorbent resulted in an additional surface area, thus increasing the available adsorption sites on the adsorbent [23]. On the contrary, as the adsorbent amount increases from 1.0 to 5.0 g (laboratory scale) and 200 to 1,000 g (pilot scale), the adsorption capacity at equilibrium decreases (183.8–58.8 mg/g for bagasse under laboratory scale; 10,859.1–2,371.6 mg/g for modified bagasse under laboratory scale; and 2,147.1–800.7 mg/g for modified bagasse under pilot scale). At a higher adsorbent dosage, a

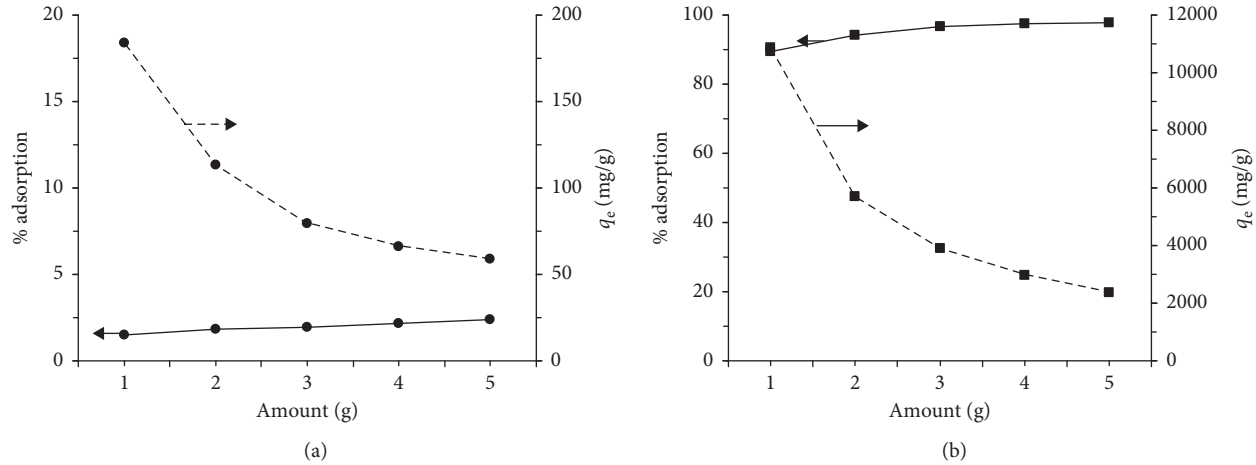

Figure 5: Graphical relationship of percent adsorption, adsorbent dosage, and adsorption capacity at equilibrium under laboratory-scale (a) bagasse and (b) modified bagasse.

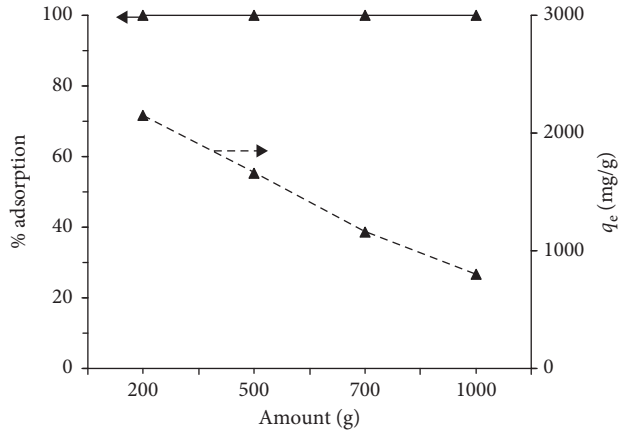

Figure 6: Graphical relationship of percent adsorption, adsorbent dosage, and adsorption capacity at equilibrium under pilot-scale setup using modified bagasse.

concentration gradient was produced wherein at the adsorbent surface, it has a higher concentration of the adsorbate compared to the concentration in the emulsion decreasing the value of the adsorption capacity at equilibrium. These results were also reported in adsorption of methylene blue dye using sewage sludge-derived biochar [24].

3.3. Models of Adsorption Isotherms. Adsorption isotherms were evaluated in order to determine the variance between the data of experimental and theoretical adsorption capacity at equilibrium. In addition, these models often provide insights into the adsorption mechanism and surface properties and affinities of the adsorbents [25]. In this study, Langmuir, Freundlich, and Temkin models were used.

Langmuir isotherm is dependent on the assumption that intermolecular forces decrease abruptly with distance and predict the existence of an adsorbate monolayer at the surface of the adsorbent; adsorption takes place at specific homogeneous sites within the adsorbent once an adsorbate occupies a site [26]. Langmuir isotherm is often used to describe adsorption of adsorbate from a liquid solution. The following equations are the nonlinear and linear forms of Langmuir isotherm, respectively:

$$q_{e,cal} = \left(\frac{q_m K_L C_e}{1 + K_L C_e}\right), \tag{9}$$

$$\frac{1}{q_{e,exp}} = \left(\frac{1}{q_m K_L}\right)\frac{1}{C_e} + \frac{1}{q_m}, \tag{10}$$

where $q_{e,cal}$ is the calculated adsorption capacity at equilibrium (mg/g), q_m is the maximum adsorption capacity (mg/g), and K_L is the free adsorption energy-based Langmuir constant (L/mg).

Based from the linear plot of $1/q_{e,exp}$, versus $1/C_e$, q_m and K_L can be calculated from its intercept and slope. Tables 1 and 2 summarize the isotherms constants of the laboratory- and pilot-scale experiments as well as the value of correlation coefficient, R^2, and the separation factor, R_L, using the modified bagasse, respectively.

Another essential Langmuir isotherm parameter is the separation factor which can be used to predict the affinity of the adsorbate to the adsorbent [27], which is expressed in the following equation:

$$R_L = \left(\frac{1}{1 + K_L C_0}\right), \tag{11}$$

where R_L is the separation factor, a dimensionless equilibrium parameter.

This parameter can indicate the type of Langmuir isotherm which follows the following conditions of irreversible ($R_L = 0$), favorable ($0 < R_L < 1$), linear ($R_L = 1$), and unfavorable ($R_L > 1$). By applying the conditions to the calculated data, it was found out that the adsorption experiment is favorable. Figures 7(a) and 7(b) show the Langmuir isotherm plots of adsorption of both laboratory- and pilot-scale system using modified bagasse.

Freundlich isotherm uses an empirical relationship to assume that the adsorption energy of a protein binding to a

Table 1: Langmuir isotherm constants using modified bagasse using a laboratory-scale system.

Adsorbent dosage (g)	$q_{e,exp}$ (mg/g)	q_m (mg/g)	K_L (L/mg)	R^2	χ^2	R_L	$q_{e,cal}$ (mg/g)
1.0	10,859.1						7,466.1
2.0	5,714.5						4,937.9
3.0	3,905.6	20,000	0.00005	0.9988	1,344.52	0.15	3,227.6
4.0	2,953.7						2,553.2
5.0	2,371.6						2,240.8

Table 2: Langmuir isotherm constants using modified bagasse using a pilot-scale system.

Adsorbent dosage (g)	$q_{e,exp}$ (mg/g)	q_m (mg/g)	K_L (L/mg)	R^2	χ^2	R_L	$q_{e,cal}$ (mg/g)
200	2,147.1						1,661.0
500	1,654.2	2,000	0.01	0.9212	141.95	0.01	1,507.4
700	1,157.3						1,295.8
1000	800.7						757.8

site is dependent on the availability of the adjacent sites. However, this isotherm is inhibited by the amount of adsorbed solute which increases indefinitely with the concentration of the solute in the solution [28]. It can be used for nonideal heterogeneous adsorption that can be expressed in a nonlinear and linear form in the following equations, respectively:

$$q_{e,cal} = K_F C_e^{1/n}, \tag{12}$$

$$\log q_{e,exp} = \log K_F + \frac{1}{n}\log C_e, \tag{13}$$

where K_F is the Freundlich isotherm constant (mg/g)·(L/mg)$^{1/n}$ and $1/n$ is the heterogeneity factor, a dimensionless number.

These parameters can be calculated using the intercept and slope of the linear plot of log q_e versus log C_e. Tables 3 and 4 summarize the isotherms constants of the laboratory- and pilot-scale experiments as well as the value of correlation coefficient, R^2. Figures 8(a) and 8(b) show the Freundlich isotherm plot of adsorption of both laboratory and pilot scales using modified bagasse.

Temkin isotherm assumes that the heat decreases linearly with uniform adsorption energy distribution and can be expressed as the following equations, for its nonlinear and linear forms [29, 30], respectively:

$$q_{e,cal} = B\ln\left(K_T C_e\right), \tag{14}$$

$$q_{e,cal} = B\ln K_T + B\ln C_e, \tag{15}$$

where B is the heat of adsorption, related to RT/b (R is the gas constant in 8.314 J/K·mol), T is the absolute temperature (K), and b is the Temkin constant, related to the heat of adsorption in J/mol, and K_T is the Temkin isotherm constant in L/g.

Tables 5 and 6 summarize the isotherms constants of the laboratory- and pilot-scale experiments as well as the value of correlation coefficient, R^2. Figures 9(a) and 9(b) show the Temkin isotherm plots of adsorption of both laboratory- and pilot-scale system using modified bagasse.

Comparing R^2 of all isotherms, it was determined that adsorption under a laboratory-scale system followed a Langmuir isotherm. whereas for a pilot-scale system, it is Freundlich isotherm. Nevertheless, calculation of R^2 was only limited to linearize forms of isotherm equations, wherein at a higher C_e value, a better fit correlation will be obtained. This is an obvious inherent bias with regards to the linearized isotherm plots [31]. Due to this bias, chi-square (χ^2) error function was employed to evaluate the

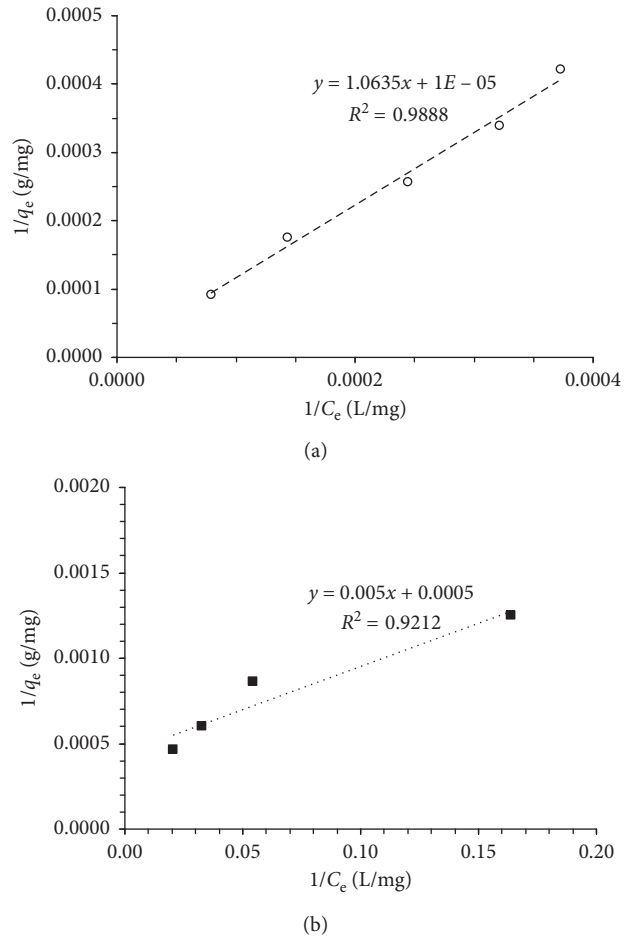

Figure 7: Langmuir isotherm plot using modified bagasse under (a) laboratory and (b) pilot scales.

Table 3: Freundlich isotherm constants using modified bagasse using a laboratory-scale system.

Adsorbent dosage (g)	$q_{e,exp}$ (mg/g)	n	K_F (mg/g)·(L/mg)$^{1/n}$	R^2	χ^2	$q_{e,cal}$ (mg/g)
1.0	10,859.1					10,642.7
2.0	5,714.5					4,947.9
3.0	3,905.6	1.07	1.52	0.9925	48.29	3,227.6
4.0	2,953.7					2,553.2
5.0	2,371.6					2,240.8

Table 4: Freundlich isotherm constants using modified bagasse using a pilot-scale system.

Adsorbent dosage (g)	$q_{e,exp}$ (mg/g)	n	K_F (mg/g)·(L/mg)$^{1/n}$	R^2	χ^2	$q_{e,cal}$ (mg/g)
200	2,147.1					2,046.1
500	1,654.2	2.11	324.6	0.9710	21.24	1,637.6
700	1,157.3					1,287.3
1000	800.7					763.6

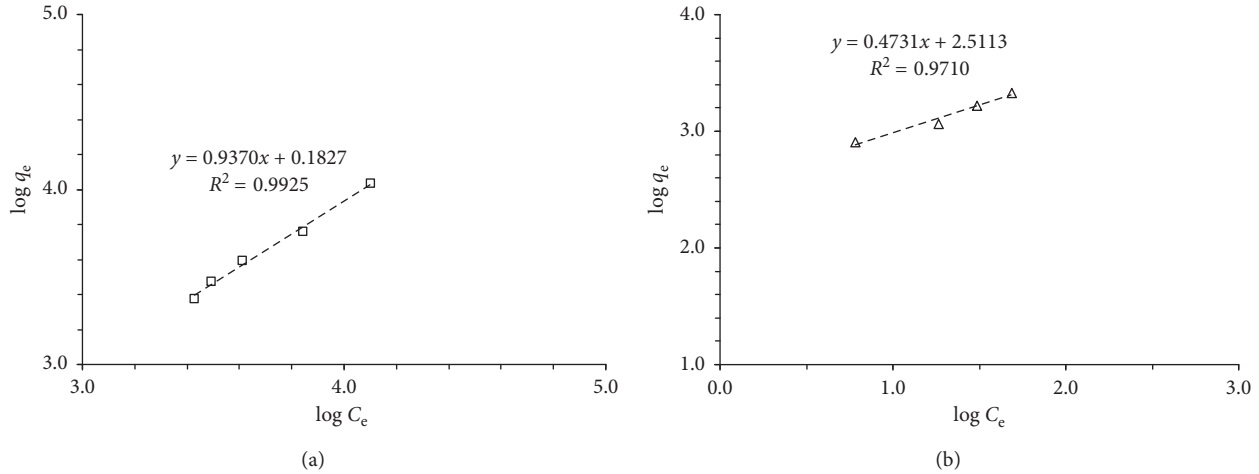

Figure 8: Freundlich isotherm plot using modified bagasse under (a) laboratory and (b) pilot scales.

Table 5: Temkin isotherm constants using modified bagasse using a laboratory-scale system.

Adsorbent dosage (g)	$q_{e,exp}$ (mg/g)	B	K_T (L/g)	R^2	χ^2	$q_{e,cal}$ (mg/g)
1.0	10,859.1					10,646.5
2.0	5,714.5					6,153.2
3.0	3,905.6	2,534.2	0.00054	0.9483	432.87	3,706.1
4.0	2,953.7					2,843.7
5.0	2,371.6					2,461.5

Table 6: Temkin isotherm constants using modified bagasse using a pilot-scale system.

Adsorbent dosage (g)	$q_{e,exp}$ (mg/g)	B	K_T (L/g)	R^2	χ^2	$q_{e,cal}$ (mg/g)
200	2,147.1					1,994.7
500	1,654.2	628.05	0.49	0.9151	71.10	1,698.9
700	1,157.3					1,379.5
1000	800.7					686.1

isotherm constant and the best fit isotherm. The chi-square error function can be calculated using the following equation:

$$\chi^2 = \sum\left[\frac{\left(q_{e,exp} - q_{e,cal}\right)^2}{q_{e,exp}}\right]. \quad (16)$$

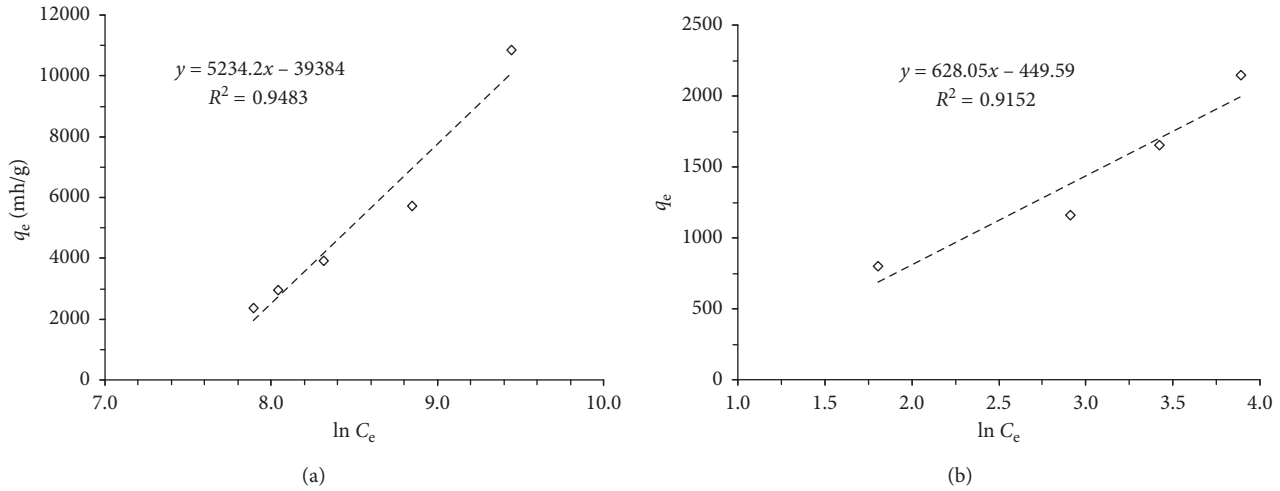

Figure 9: Temkin isotherm plot using modified bagasse under (a) laboratory and (b) pilot scales.

Comparing chi-square error value of each isotherm, it was found out that, at both systems of laboratory- and pilot-scale setup, it followed a Freundlich isotherm. As a result, the Freundlich isotherm fitted the experimental data very well; thus, surface heterogeneity and/or pore size of the modified bagasse played an important and significant role in the adsorption of CFW [32]. Figures 10(a) and 10(b) show the experimental and theoretical plots of Langmuir, Freundlich, and Temkin isotherms using laboratory- and pilot-scale systems.

3.4. Batch Design. Adsorption isotherm relations were used to predict the design of the single-stage batch adsorption systems. Figure 11 shows the schematic diagram of the batch design.

An inlet stream of the emulsion, V (L) with an initial concentration of C_0 in mg/L was reduced to a final concentration of C_1 in mg/L using M as the adsorbent dosage with an initial adsorbate concentration of q_0 in mg/g. When the adsorption takes place, the adsorbate concentration of the adsorbent increases from q_0 to q_1. Applying the mass balance equation for the adsorption system can be written as follows [33]:

$$V(C_0 - C_1) = M(q_0 - q_1). \quad (17)$$

Using fresh adsorbent, q_0 will be equal to zero; thus, equation (17) will be reduced to the following equation:

$$V(C_0 - C_1) = M(q_1). \quad (18)$$

Under equilibrium conditions, C_1 will be equal to C_e and q_1 will be equal to q_e (substituted to equation (18)). Since this study confirmed the best fit model was the Freundlich isotherm, equation (12) was introduced to equation (18) at equilibrium conditions, and by rearranging, the following equation was derived:

$$\frac{M}{V} = \frac{(C_0 - C_e)}{K_F C_e^{1/n}}. \quad (19)$$

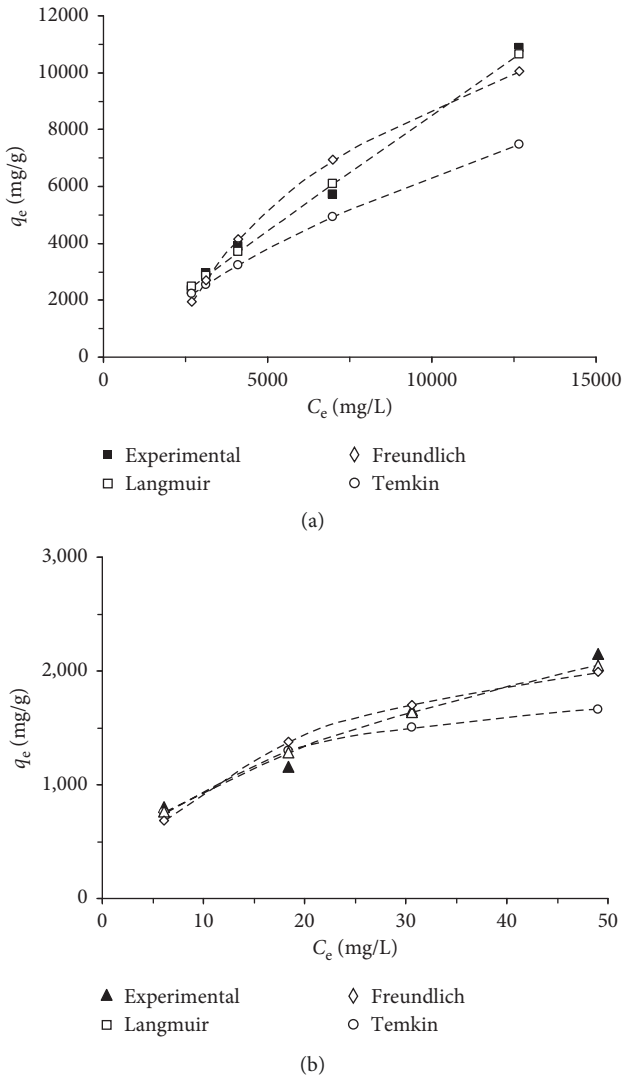

Figure 10: Adsorption of CFW to the modified bagasse under (a) laboratory and (b) pilot scales.

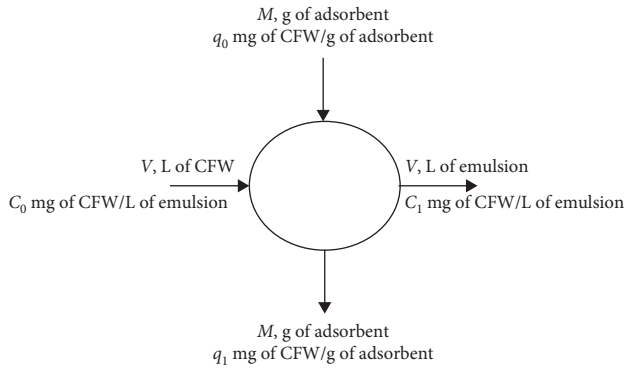

Figure 11: Single-stage batch adsorption design.

Equation (19) permits the analytical calculation of the adsorbent emulsion ratio for a given change in emulsion concentration, C_0 (5,000 mg/L) to CC_e (2.5 mg/L). Figure 12 shows the relationship of the adsorbent dosage and CFW volume that was derived from equation (19). For a liter of CFW, 10.2 g and 59.2 g of the modified bagasse are required under laboratory- and pilot-scale systems, respectively.

3.5. Scanning Electron Microscope. Figures 13(a) and 13(b) show the surface morphologies of the fiber of modified bagasse before and after adsorption CFW. From Figure 13(a), pendant flakes of aluminum sulfate were observed covering almost the entire surface area of the modified bagasse fiber. On the contrary, Figure 13(b) shows an enlarged modified bagasse fiber with corrugation and creases at the surface. This indicates that the CFW was adsorbed on the surface of modified bagasse.

3.6. Fourier-Transform Infrared Spectroscopy. Figures 14(a)–14(c) show the IR spectra of the modified bagasse, CFW, and modified bagasse after adsorption, respectively. Based from the IR spectra of the CFW, an alkane, methylene, and methyl groups were confirmed by the appearance of peaks at 2,925 and 2,855 cm^{-1}, 1,465 cm^{-1}, and 1,375 cm^{-1}, respectively. The long chain methylene group containing more than four carbon atoms appeared at 720 cm^{-1} [34]. On the contrary, the IR spectra of the modified bagasse after adsorption includes the presence of alkane at 2,927 and 2,869 cm^{-1}, methylene group at 1,468 cm^{-1}, and methyl group at 1,379 cm^{-1}. The appearance of these functional groups indicated that CFW adhered to the surface of the adsorbent.

3.7. Heat of Combustion and Proximate Analysis. After the adsorption process, the heat of combustion of the modified bagasse was higher compared to the values measured before adsorption. However, the calculated heat of combustion of the adsorbent after adsorption using both laboratory and pilot scales was relatively lower to that of the experimental heat value of coal, having values of 13.61, 14.85, and 17.6 kJ/g [35]. Nevertheless, the measured heat value of the adsorbent was significant enough for it to be considered and utilized as solid fuel.

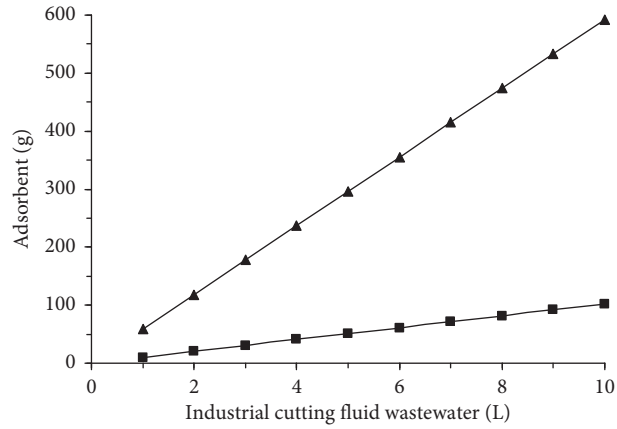

Figure 12: Adsorbent dosage versus CFW volume under laboratory (■) and pilot (▲) scales.

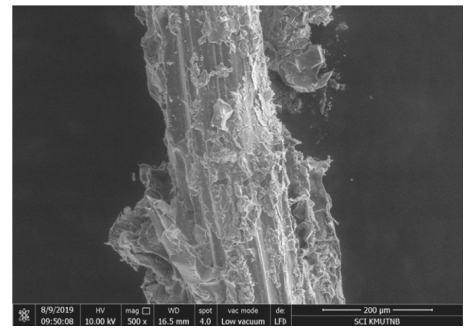

(a)

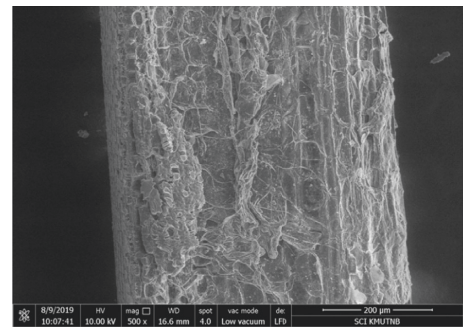

(b)

Figure 13: Surface morphology of modified bagasse: (a) before and (b) after the adsorption of CFW.

The compositions of the adsorbent were analyzed using the proximate analysis. Moisture, ash, volatile matter, and fixed carbon were measured from bagasse and modified bagasse both before adsorption and modified bagasse after adsorption under both systems. It was found out that the increase in the moisture content of the adsorbent after adsorption lowered the heat and efficiency of combustion. Also, a high volatile matter content ignites easily; however, after adsorption, the ignition occurred slowly. There is also a significant decrease in the ash content of the adsorbent right after adsorption resulted in a decreased residue. Due to an increased fixed carbon content of the adsorbent after adsorption, it will need a longer combustion time. Table 7

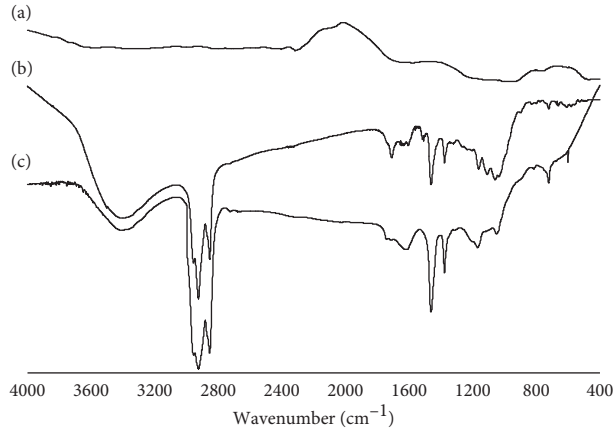

Figure 14: FTIR spectra of (a) modified bagasse, (b) CFW, and (c) modified bagasse after adsorption.

Table 7: Heat of combustion and proximate analysis.

Adsorption		ΔH (kJ/g)	% moisture	% volatile matter	% ash	% fixed carbon
Before	Bagasse	13.12	6.0	85.1	3.4	5.5
	Modified bagasse	10.17	10.6	64.3	19.4	5.7
After	Modified bagasse (laboratory)	23.78	21.9	47.7	2.1	28.3
	Modified bagasse (pilot)	25.02	21.3	51.7	3.5	23.5

summarizes the measured values of heat and proximate analysis.

A change in the value of the heat of combustion of a material indicates a variation with its physical or chemical properties. In this experiment, the heat of combustion of the modified bagasse significantly increased to 25.02 kJ/kg from 10.17 kJ/kg after the adsorption process. The difference between these values arises from the adsorption of adsorbate molecules. Considering the final value for the heat of combustion, the modified bagasse after the adsorption process can be used as a solid fuel.

4. Conclusions

The properties measured on the adsorption of industrial cutting fluid wastewater (CFW) using bagasse and modified bagasse validate the feasibility of using an organic biomass adsorbent. The point of zero charge of the bagasse and the modified bagasse was measured to be at pH 5.5 and 2.4, respectively. Increasing the adsorbent dosage (both for laboratory scale using bagasse and modified bagasse; both for laboratory scale and pilot scale using modified bagasse) resulted in an increase in the percent adsorption due to the increase in the number of available adsorption sites on the adsorbent. However, there was a decrease in the adsorption capacity at equilibrium since at higher adsorbent dosage, a concentration gradient was produced at the adsorbent surface. In addition, it was determined that the best fitted model for both systems (laboratory and pilot scales) were the Freundlich isotherm. Thus, in adsorbing CFW, the surface heterogeneity as well as the pore size of the modified bagasse played a significant role. It was also determined through experiments that, for every liter of CFW, 10.2 g and 59.2 g of the modified bagasse are required under laboratory- and pilot-scale systems, respectively. In terms of the measured heat value, the modified bagasse was higher compared to the values measured before adsorption and significant enough for it to be considered as a solid fuel. The functional groups were verified using the FTIR analysis. The adsorption of the CFW is visible based on the SEM micrographs. The combustion of the adsorbent was analyzed using proximate analysis before (bagasse and modified bagasse) and after (modified bagasse under a laboratory and pilot scale) adsorption. The moisture content and the fixed carbon of the adsorbent after adsorption increased lowering the heat and efficiency of combustion and will require a longer combustion time. On the contrary, the ignition occurred slowly and there was a reduction of residue after combustion due to the decrease in the volatile content and ash content, respectively. Thus, the bagasse and modified bagasse under laboratory- and pilot-scale systems are viable materials for the adsorption of CFW and to be considered as solid fuel.

Data Availability

The adsorption data used to support the findings of this study are included within the article.

Conflicts of Interest

The authors declare that there are no conflicts of interest regarding the publication of this paper.

Acknowledgments

This research was funded by King Mongkut's University of Technology North Bangkok (Contract no. KMUTNB-ART-60-024).

References

[1] J. M. Benito, A. Cambiella, A. Lobo, G. Gutiérrez, J. Coca, and C. Pazos, "Formulation, characterization and treatment of metalworking oil-in-water emulsions," *Clean Technologies and Environmental Policy*, vol. 12, no. 1, pp. 31–41, 2010.

[2] P. Yan, Y. Rong, and G. Wang, "The effect of cutting fluids applied in metal cutting process," *Proceedings of the Institution of Mechanical Engineers, Part B: Journal of Engineering Manufacture*, vol. 230, no. 1, pp. 19–37, 2016.

[3] J. P. Byers, *Metalworking Fluids*, Taylor & Francis, Boca Raton, FL, USA, 2nd Edition, 2006

[4] M. Schwarz, M. Dado, R. Hnilica, and D. Veverková, "Environmental and health aspects of metalworking fluid use," *Polish Journal of Environmental Studies*, vol. 24, no. 1, pp. 37–45, 2015.

[5] C. Cheng, D. Phipps, and R. M. Alkhaddar, "Treatment of spent metalworking fluids," *Water Research*, vol. 39, no. 17, pp. 4051–4063, 2005.

[6] T. Viraraghavan and G. N. Mathavan, "Treatment of oil-in-water emulsions using peat," *Oil and Chemical Pollution*, vol. 4, no. 4, pp. 261–280, 1988.

[7] G. N. Mathavan and T. Viraraghavan, "Use of peat in the treatment of oily waters," *Water, Air, & Soil Pollution*, vol. 45, no. 1-2, pp. 17–26, 1989.

[8] G. N. Mathavan and T. Viraraghavan, "Coalescence/filtration of an oil-in-water emulsion in a peat bed," *Water Research*, vol. 26, no. 1, pp. 91–98, 1992.

[9] C. Solisio, A. Lodi, A. Converti, and M. D. Borghi, "Removal of exhausted oils by adsorption on mixed Ca and Mg oxides," *Water Research*, vol. 36, no. 4, pp. 899–904, 2002.

[10] A. Cambiella, E. Ortea, G. Rios, J. Benito, C. Pozos, and J. Coca, "Treatment of oil-in-water emulsions: performance of a sawdust bed filter," *Journal of Hazardous Materials*, vol. 131, no. 1–3, pp. 195–199, 2006.

[11] K. Piyamongkala, L. Mekasut, and S. Pongstabodee, "Cutting fluid effluent removal by adsorption on chitosan and sds-modified chitosan," *Macromolecular Research*, vol. 16, no. 6, pp. 492–502, 2008.

[12] S. Ibrahim, H.-M. Ang, and S. Wang, "Removal of emulsified food and mineral oils from wastewater using surfactant modified barley straw," *Bioresource Technology*, vol. 100, no. 23, pp. 5744–5749, 2009.

[13] A. R. Tembhurka and R. Deshpande, "Powdered activated lamon peels as adsorbent for removal of cutting oil from wastewater," *Journal of Hazardous, Toxic, and Radioactive Waste*, vol. 16, no. 4, pp. 311–315, 2012.

[14] http://www.ocsb.go.th/th/cms/detail.php?ID=142&SystemModuleKey=production.

[15] P. L. Homagai, K. N. Ghimire, and K. Inoue, "Adsorption behavior of heavy metals onto chemically modified sugarcane bagasse," *Bioresource Technology*, vol. 101, no. 6, pp. 2067–2069, 2010.

[16] A. Bhatnagar and M. Sillanpää, "Utilization of agro-industrial and municipal waste materials as potential adsorbents for water treatment," *Chemical Engineering Journal*, vol. 157, no. 2-3, pp. 277–296, 2010.

[17] K. Piyamongkala and T. Chanpattanapong, Thai Petty Patent No 950, 2015, http://patentsearch.ipthailand.go.th/DIP2013/view_public_data.php?appno=11428700138.

[18] W. Champreecha, A. Pranudta, and K. Piyamongkala, "Equilibrium and batch design studies for cutting fluid adsorption onto sugarcane bagasse and modified sugarcane bagasse," *The Journal of King Mongkut's University of Technology North Bangkok*, vol. 27, no. 1, pp. 1–13, 2017.

[19] Y. Jiang, H. Pang, and B. Liao, "Removal of copper(II) ions from aqueous solution by modified bagasse," *Journal of Hazardous Materials*, vol. 164, no. 1, pp. 1–9, 2009.

[20] A. Pinotti and N. Zaritzky, "Effect of aluminum sulfate and cationic polyelectrolytes on the destabilization of emulsified wastes," *Waste Management*, vol. 21, no. 6, pp. 535–542, 2001.

[21] O. A. A. Eletta, O. A. Ajayi, O. O. Ogunleye, and I. C. Akpan, "Adsorption of cyanide from aqueous solution using calcinated eggshells: equilibrium and optimisation studies," *Journal of Environmental Chemical Engineering*, vol. 4, no. 1, pp. 1367–1375, 2016.

[22] J. E. Anderson, B. R. Kim, S. A. Mueller, and T. V. Lofton, "Composition and analysis of mineral oils and other organic compounds in metalworking and hydraulic fluids," *Critical Reviews in Environmental Science and Technology*, vol. 33, no. 1, pp. 73–109, 2003.

[23] A. M. Aljeboree, A. N. Alshirifi, and A. F. Alkaim, "Kinetics and equilibrium study for the adsorption of textile dyes on coconut shell activated carbon," *Arabian Journal of Chemistry*, vol. 10, no. 2, pp. 3381–3393, 2017.

[24] S. Fan, Y. Wang, Z. Wang, J. Tang, J. Tang, and X. Li, "Removal of methylene blue from aqueous solution by sewage sludge-derived biochar: adsorption kinetics, equilibrium, thermodynamics and mechanism," *Journal of Environmental Chemical Engineering*, vol. 5, no. 1, pp. 601–611, 2017.

[25] Y.-S. Ho, W.-T. Chiu, and C.-C. Wang, "Regression analysis for the sorption isotherms of basic dyes on sugarcane dust," *Bioresource Technology*, vol. 96, no. 11, pp. 1285–1291, 2005.

[26] Y. C. Wong, Y. S. Szeto, W. H. Cheung, and G. McKay, "Equilibrium studies for acid dye adsorption onto chitosan," *Langmuir*, vol. 19, no. 19, pp. 7888–7894, 2003.

[27] H. Hassan, A. Salama, A. K. El-Ziaty, and M. El-Sakhawy, "New chitosan/silica/zinc oxide nanocomposite as adsorbent for dye removal," *International Journal of Biological Macromolecules*, vol. 131, pp. 520–526, 2019.

[28] Z. Eren and F. N. Acar, "Equilibrium and kinetic mechanism for reactive black 5 sorption onto high lime soma fly ash," *Journal of Hazardous Materials*, vol. 143, no. 1-2, pp. 226–232, 2007.

[29] I. D. Mall, V. C. Srivastava, and N. K. Agarwal, "Removal of orange-G and methyl violet dyes by adsorption onto bagasse fly ash-kinetic study and equilibrium isotherm analyses," *Dyes and Pigments*, vol. 69, no. 3, pp. 210–223, 2006.

[30] S. Rengaraj, J.-W. Yeon, K. Kim, Y. Jung, Y. K. Ha, and W.-H. Kim, "Adsorption characteristics of Cu(II) onto ion exchange resin 252H and 1500H: kinetics, isotherms and error analysis," *Journal of Hazardous Materials*, vol. 143, no. 1-2, pp. 469–477, 2007.

[31] Y. C. Wong, Y. S. Szeto, W. H. Cheung, and G. McKay, "Adsorption of acid dyes on chitosan-equilibrium isotherm analyses," *Process Biochemistry*, vol. 39, no. 6, pp. 695–704, 2004.

[32] S. Wang, Y. Boyjoo, and A. Choueib, "A comparative study of dye removal using fly ash treated by different methods," *Chemosphere*, vol. 60, no. 10, pp. 1401–1407, 2005.

[33] P. S. Kumar, S. Ramalingam, V. Sathyaselvabala, S. D. Kirupha, A. Murugesan, and S. Sivanesan, "Removal of cadmium(II) from aqueous solution by agricultural waste cashew nut shell," *Korean Journal of Chemical Engineering*, vol. 29, no. 6, pp. 756–768, 2012.

[34] D. L. Pavia, G. M. Lampman, and G. S. Kriz, *Introduction to Spectroscopy*, Harcourt, Orlando, FL, USA, 2001.

[35] N. E. Altun, M. V. Kök, and C. Hicyilmaz, "Effect of different binders on the combustion properties of lignite. Part II. Effect on kinetics," *Journal of Thermal Analysis and Calorimetry*, vol. 65, no. 3, pp. 797–804, 2001.